Jour. Fac. Sci., Hokkaido Univ., Ser. VII (Geophysics), Vol. 11, No. 1, 117-133, 1998.

Features on Snow Clouds Derived from AVHRR/NOAA and Doppler Radar : Broad Band Cloud off the West Coast of Hokkaido Island

Naonori Osaki, Hiroshi Uyeda and Katsuhiro Kikuchi

Division of Earth and Planetary Sciences, Graduate School of Science, Hokkaido University, Sapporo 060-0810, Japan

(Received November 30, 1997)

Abstract

Initial structures and cloud systems of a broad band snow cloud (BBC) formed off Hokkaido Island, Japan are investigated by AVHRR/NOAA-10 and single X-band Doppler radar data. The present paper has examined a method to distinguish convective cells and anvils of snow clouds in the BBC using satellite radiances. The procedure presents utilizing an actual scatter diagram corresponding to the brightness temperature differences (T3-T4) of the AVHRR/NOAA-10 channels 3 and 4 plotted as the function of channel 4 brightness temperature (T4). On the basis of the theoretically radiative background, the radiative characteristics of a snow cloud and BBC are compared with their cloud systems.

Radiative features of snow clouds acquired over the Japan Sea on 28 January 1991 are diagnosed, as results of the observation and the application of the present procedure. The alignment of strong echoes over 20 dBZ corresponds to the region of the lower T4. The convective regions perform the T3-T4 value yields close to 0 K ($\pm$1 K). Also, radiative properties of snow clouds to the northern and southern parts outside of the BBC are diagnosed. The radiation characteristics of the northern region are attributed to the strong streak clouds under the winter monsoon outbreak with predominant cirrus and/or cold anvil regions including convective cells. The southern region is comprised of convective snow clouds. The significant differences in radiative properties between the northern and southern regions outside of the BBC are considered to mirror the stages of cloud developments and/or the depth of mixing layers. Therefore, the thickness of the layers in the northern region is larger than that in the southern region.

The comparison of radiative features in different regions near the BBC revealed the conformity of convective radiation attributions and a strong radar reflectivity, suggesting that the present application is exceedingly effective to identify the convective snow cloud and to estimate a cloud development stage.

1. Introduction

Cloud and radiation interactions have long been considered to reveal one of the key problems in meso-scale research. The relation between clouds and radiations have become even more crucial as several sensitivity studies (for instance, Liou, 1980 ; Liou, 1992) have shown that the response of theoretical and numerical models was extremely dependent on the various hypotheses and parameterizations used to simulate a process. However, research on meso-scale cloud systems and radiative properties is rarely performed, although it is well investigated on planetary scale schemes. We focus on snow cloud systems including various scenes of dynamic features influencing their own radiances at a cloud-top. For the meso-scale cloud systems, snow clouds are the major presence in a high-latitude region.

In the winter monsoon, various meteorological observations have been carried out on the west coast of the Japan Sea to inquire into the formation system (and its mechanism) of snow clouds. Mesoscale disturbances frequently appear over both the northern and central parts of Japan Sea (Kodama et al., 1995) along the JPCZ (the Japan-Sea Polar airmass Convergence Zone) according to Asai (1988). Also a broad band snow cloud (hereafter BBC) extending from north to south is occasionally formed off the western coast of Hokkaido Island. The representative BBC has a scale of 500～1000 km in length and 50 ～200 km in width, is maintained for 1～2 days, and generates heavy snowfalls when it lands (Okabayashi and Satomi, 1971). In recent years, Doppler radar observations (Fujiyoshi et al., 1988 ; Tsuboki et al., 1989 ; Satoh et al., 1992) and numerical simulations (Sasaki and Satomura, 1991 ; Nagata, 1993) of the BBC have been accomplished. It is widely recognized that the BBC commonly originates on the western side of Soya Straits according to detailed analyses of satellite imageries (Katsumata et al., 1996). The cold air that passes through the Soya Straits from east to west is suggested to be one of the initial disturbances triggering the evolution of the BBC (Kobayashi et al., 1987).

The detailed dynamic and kinematic structures of the BBC as a meso-scale phenomenon, comparable with the radiative properties, has not yet been investigated. In the present paper, firstly, the relationship between the brightness temperature of NOAA polar-orbiting satellite data and X-band Doppler radar reflectivity data are explored. On the basis of the above results, the radiative characteristics of a snow cloud and BBC are compared with their cloud systems.

2. Observations and data

Radar observations were carried out from 16 to 28 January 1991 on Rebun Island (45°28′N, 140°58′E) in the northern part of Hokkaido, Japan as shown in Fig. 1. Rebun Island is located in the Japan Sea nearly 60 km away from the western coast of Wakkanai. The observation site is an appropriate point to scrutinize the snow cloud without the modification of orographic effects during winter monsoon surges, since it is surrounded in the ocean. The characteristics of radar echoes and meso-β-scale structure on the BBC during this observation period are reported by Uyeda et al. (1992) and Takemoto et al. (1998).

The single X-band Doppler radar (Meteorological Laboratory Radar of Hokkaido University) was installed at the Cape Sukoton in Rebun Island. An analysis area including Rebun Island is illustrated in Fig. 1. The area depended on the NOAA (U.S. National Oceanic and Atmospheric Administration) polar-orbiting satellite is shown in the larger box of the left panel in Fig. 1. The box covers 1024×1024 pixels of satellite images. In the right panel of Fig. 1, the box includes 128×128 pixels of detailed NOAA imageries and the circle of 60 km in radius indicates the coverage of Doppler radar observations. The field, the box of 128×128 pixels, is drawn from original NOAA imagery with 1024×1024 pixels, represented in the right panel in Fig. 1 constructs the comparison of satellite and radar.

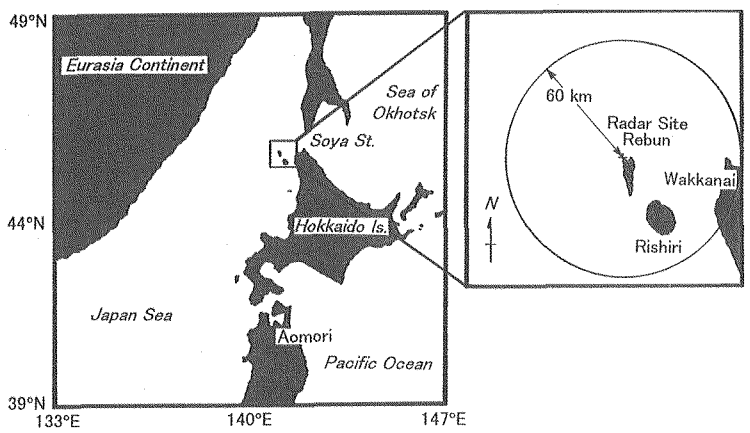

Fig. 1. Map for the observation and analysis area. The larger box in left panel is 1024×1024 pixels with AVHRR/NOAA-10 satellite imagery. In the right panel around Rebun Island, the box covers 128×128 pixels of the satellite imagery. The cross and the circle of 60 km in radius represent the single X-Band Doppler radar site (Cape Sukoton) and the observation coverage respectively.

The satellite data set (provided by the Center for Atmospheric and Oceanic Studies, Faculty of Science, Tohoku University) utilized in this analysis is channels 2, 3 and 4 of the AVHRR (the Advanced Very High Resolution Radiometer) instrument on board the NOAA-10 satellite. These channels for AVHRR/NOAA-10 are in the following wavelength (Kidder and Vonder Harr, 1995):

- the solar spectrum (VIS) between 0.75 and 1.10 μm (channel 2),
- the near infrared region (NIR) between 3.55 and 3.93 μm (centered 3.7 μm ; channel 3) and
- the infrared window region (IR) between 10.5 and 11.5 μm (centered 11.0 μm ; channel 4).

Specifically, the AVHRR/NOAA HRPT (High-Resolution Picture Transmission) data set corresponding to approximately 1.1×1.1 km resolution at the subsatellite point is sufficient for detecting radiative properties and the structure of the BBC that causes severe snowfalls in the winter monsoon duration.

3. Theory and method

In general terms, detection of snow clouds on satellite images depends on the contrast between the clouds and their background. The estimation of precipitation from VIS and IR satellite data has been used to support a variety of applications (Arkin, 1979 ; Adler and Negri, 1988). These include climatology, hydrology, flush flood identification, input to agricultural models, verification of weather modification experiments and the study of convective systems. At VIS wavelengths the contrast is in terms of reflectance differences, and at infrared wavelengths the contrast is in terms of differences in brightness temperature which includes the effects of emmittance and thermodynamic temperature (Lauritson et al., 1979). For near infrared wavelengths (AVHRR/NOAA-10 channel 3) the contrast is a mixture of reflectance and brightness temperature differences. The following sections present the theoretical foundation for the algorithm developed in this paper. Included here is a discussion of the reflective thermal characteristics of the features to be analyzed.

3.1 Channel 3 radiance

The AVHRR/NOAA-10 channel 3 radiance is comprised of both reflection and emission contributions. The analysis technique requires solar reflection from channel 3 so the thermal emission contribution must be removed. For more reflective surfaces (such as water clouds), solar reflection is the greater

contributor to the channel 3 radiance measurement. On the channel 3, the measured radiance is expressed by:

$$L_3=\varepsilon_3 B_3(T)+\gamma_3(\theta_0,\theta,\phi)L_0\cos\theta_0 \ . \tag{1}$$

The first term on the right hand side is the contribution to the measured radiance from thermal emission of the viewed surface assuming the transmittance of the intervening atmosphere is equal to 1.0. The second term on the right hand side is the contribution to the measured radiance due to solar reflection. The amount of reflected solar radiance reaching the satellite is determined by the incident solar radiance (L_0) that is weighted by the cosine of the solar zenith angle (θ_0), and the reflectance (γ) of the viewed surface. The directional reflectance is a function of the solar zenith angle, the satellite zenith angle (θ), and the relative azimuth angle between them (ϕ). Hemispherical reflectance is related to the directional reflectance factor (ξ). These relationships are expressed as (Taylor and Stowe, 1984):

$$\rho_3=\gamma_3(\theta_0,\theta,\phi)/\xi \ . \tag{2}$$

Thermal emission for channel 3 was estimated by inverting the Planck function to find the temperature corresponding to the channel 4 radiance measurement. This temperature was then used to solve the Planck function for channel 3 ($B_3(T)$). An emittance (ε_3) for channel 3 is related to reflectance (ρ_3) according to Kirchhoff's law and shown by

$$\varepsilon_3=1-\rho_3 \ . \tag{3}$$

Here, substituting Eqs.(2) and (3) into Eq.(1) gives the calculated radiance as expressed by:

$$L_3=(1-\rho_3)B_3(T)+\rho_3\xi L_0\cos\theta_0 \ . \tag{4}$$

Finally, solving Eq.(4) for the reflectance of the AVHRR/NOAA-10 channel 3 gives

$$\rho_3=\frac{L_3-B_3(T)}{\xi L_0\cos\theta_0-B_3(T)} \ . \tag{5}$$

Equation (5) was employed to evaluate the effective of the channel 3 reflectance for each AVHRR/NOAA-10 satellite scenes for the following analysis.

3.2 Brightness temperature differences on channel 3 and 4

The discussion before section 3.1 shows that the reflective properties on snow clouds are similar for wavelengths of the AVHRR/NOAA channel 3 and 4. Also, thin cirrus and/or anvil and convective clouds may have similar

emission characteristics. Therefore, there are some cases where a thresholding technique will fail to separate them correctly. Allen et al. (1990) expressed that there is a difference in the transmissive features of cirrus clouds between 3.7 μm and 11.0 μm. This difference is demonstrated as a brightness temperature difference between channel 3 and 4 of the AVHRR/NOAA-10. The Planck blackbody emission, as a function of temperature, varies differently for these two channels, and cirrus and/or anvil transmit more surface radiation at 3.7 μm than at 11.0 μm. Specifically, the satellite measured radiance in channel 4 is then primarily due to emission from the cloud-top. Thus the radiance in channel 4 is recognized as the cloud-top temperature, since most of the BBC is the convective system of a cumulus cloud.

The physical basis of the methods suggested by Inoue (1985), Wu (1987) and Giraud et al. (1997) was quite similar. They established that cirrus cloud-top temperature and IR effective emmissivity could be derived from two window channels centered at 11.0 μm and 12.0 μm of AVHRR/NOAA. According to these authors, 1) the brightness temperature differences of two channels are always more important for cirrus and/or anvil clouds than for thick or clear-sky areas and 2) this difference is very sensitive to the clouds' radiative and dynamic properties. Further investigations of the information content and physical meaning of the brightness temperature differences between 3.7 μm and 11.0 μm of the radiometer have led to the development of an automatic procedure for global estimates of both the cirrus and/or anvil clouds' temperature and of the ratio of the equivalent absorption coefficients in the two channels, accounting for scattering effects.

Figure 2, which corresponds to observations performed over a snow cloud-top, is employed to an example of an actual diagram of 200 AVHRR/NOAA-10 pixels and described brightness temperature differences T3-T4 (K) plotted as a function of T4 (expressing the equivalent blackbody temperature for the channel 4). For the theoretically radiative background, *Sector C* in Fig. 2 indicates the convective clouds and/or regions, as the emmissivity nearly equals 1.0 (the T3-T4 is 0 ± 1 K). *Sector A* in Fig. 2 also shows the cirrus and/or anvil clouds, since the T3-T4 yields a negative value such as Yamanouchi et al. (1987) presented in high-latitude and polar regions. Note that this negative value for the *Sector A* appears, only when T4 ranges are less than 258 K. Accordingly, the plot of the diagram denoted *Sector B* in Fig. 2 corresponds to pixels totally covering the coldest snow clouds with variety of a microphysical index (Giraud et al., 1997).

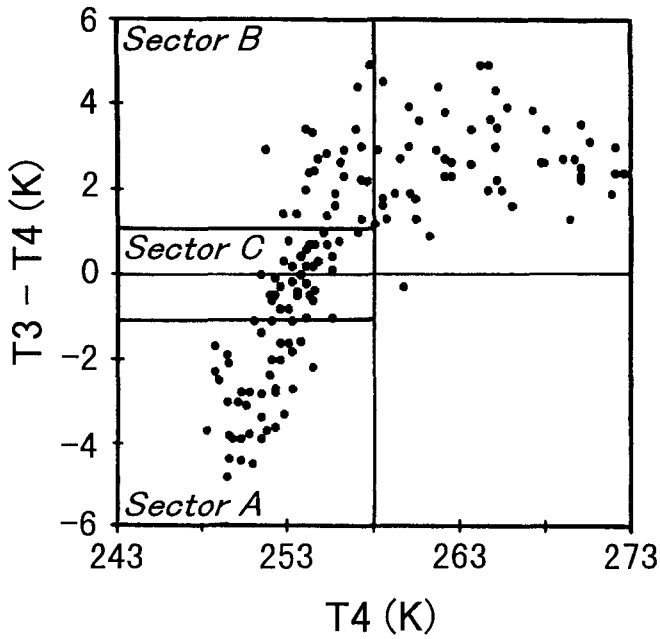

Fig. 2. Example for the scatter diagram of actually observed brightness temperature differences on channels 3 and 4; T3-T4 (K) versus the brightness temperature on channel 4; T4 (K) for 200 AVHRR/NOAA-10 pixels. *Sector A* shows the regions (the T3-T4 is less than −1 K) of the cirrus and/or anvil clouds. *Sector B* (the T3-T4 is larger than 1 K) corresponds to pixels totally covered the coldest snow clouds with the variety of a microphysical index (Giraud et al., 1997). *Sector C* indicates the convective clouds and/or regions, as the emmissivity nearly equals 1.0 (the T3-T4 yields 0±1 K).

4. Results

4.1 Synoptic situation on 28 January 1991

A typical case on 28 January 1991 is acquainted with this paper, since the BBC also appears on 23 January 1991 during the observation. Sea surface and upper level charts at 09 JST on 28 January 1991 are illustrated in Fig. 3. Although a pressure pattern presents that the northwesterly winter monsoon is prominent around Japan, isobaric lines in Fig. 3(a) are in the direction on NE-SW on the western side of Hokkaido Island and change to NW-SE on the western side of Aomori. The western coast of Hokkaido is at the rear side of a mainly low pressure area, the center of which is situated over the Sea of Okhotsk. In Fig. 3(b), a significant cold air mass which is below −12°C at 850 hPa covered Hokkaido Island. The cold vortex with temperatures lower

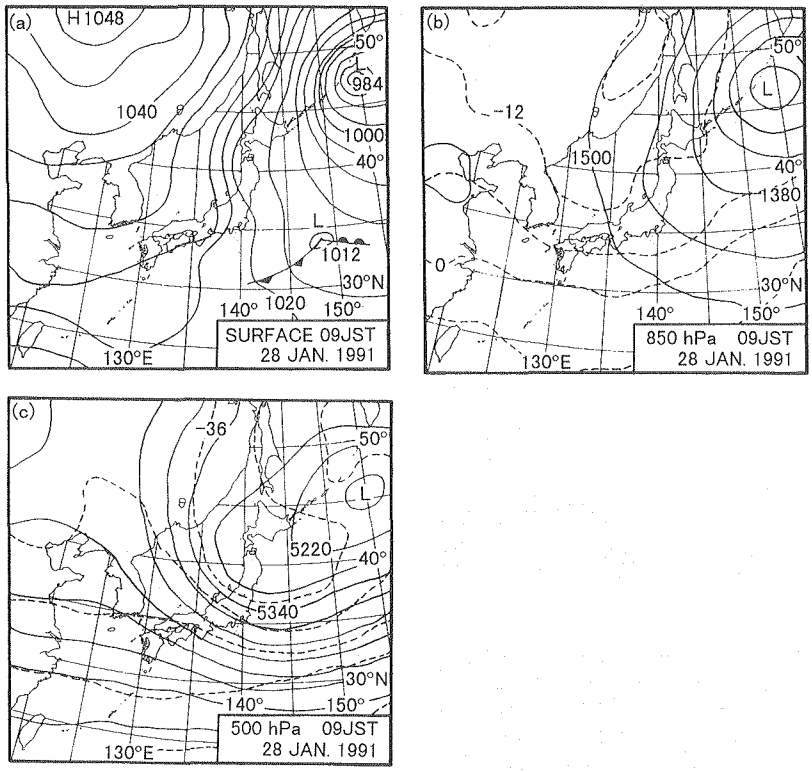

Fig. 3. Weather charts around Japan at 09 JST on 28 January 1991. (**a**). Sea surface pressure (hPa). (**b**). 850 hPa level chart with height (solid contours; m) and temperature (dashed contours; °C). (**c**). 500 hPa level chart with height (solid contours; m) and temperature (dashed contours; °C).

than −36°C at 500 hPa is located in the northern part of the jet stream in Fig. 3(c). Variations in temperature and wind on the ground at the radar site (Rebun Island) are shown in Fig. 4 when the BBC generated. The part attaching an arrow indicates the time when the BBC is confirmed by NOAA satellite images. Temperature decreases about 2°C and wind velocity is recorded as 10~15 m/s, although the wind direction tends to the north and northeast at this time. Specifically, the above synoptic conditions are consistent with those reported by other researchers (for instance, Kobayashi et al., 1987; Fujiyoshi et al., 1996) when a BBC was observed to form off the western side of Hokkaido Island.

4.2 AVHRR/NOAA-10 and X-band radar properties

The AVHRR/NOAA-10 channel 4 imagery at 0646 JST on 28 January 1991

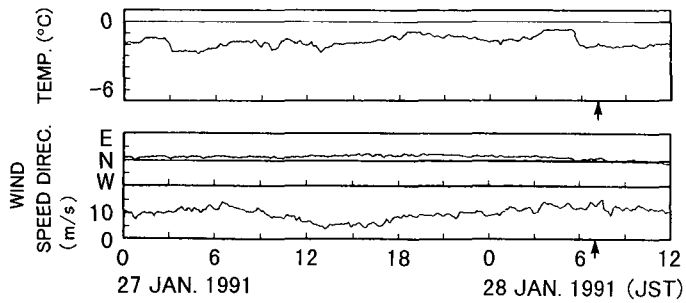

Fig. 4. Time series of temperature (°C), wind direction and speed (m/s) on the ground at the radar site (Rebun Island). An arrow indicates the time when the BBC was identified by AVHRR/NOAA-10 channel 4 (IR) imagery.

is described in Fig. 5 for the same region of Fig. 1 (left panel). The band-shaped region of low T4 is recognized in the central part over the Japan Sea in the figure with typical cloud streaks around it. The radar observation range was in the generation region of the BBC extending approximately 500 km to the western coast of Aomori. The detailed IR imagery regarding the occurrence of the BBC is represented in Fig. 6 as the same area of Fig. 1 (right panel). The low T4 region in the northwest and northeast of Rebun Island details a band-shaped cloud developing to the south which originates around the radar site.

On the other hand, the X-band Doppler radar reflectivity (dBZ) of PPI (Plan Position Indicator) with on elevation angle of 1.9° is illustrated in Fig. 7. The times at 0636 JST and 0651 JST on 28 January 1991 are the nearest AVHRR/NOAA-10 satellite scanning over the radar site. The PPI reflectivity contours in Fig. 7 are drawn for 20 dBZ (outer) and 26 dBZ (inner). The snow echoes aligned N-S over the Rebun Island at these times. The radar echoes on the PPI consist of several convective cells. This configuration is clearly coincident with the AVHRR/NOAA-10 T4 imagery in Fig. 6. Specifically, the alignment of a strong echo over 20 dBZ corresponds with the region of the lower satellite T4.

Next, in order to understand the relations between the radiative properties on the cloud-top and its cloud systems, the vertical cross section of the southwardly echo cells is inspected. Figure 8 shows the vertical cross section (an azimuth angle is 185.9°); both of the brightness temperature differences (T3-T4) on AVHRR/NOAA-10 and the RHI (Range Height Indicator) of the radar with the reflectivity (dBZ) and the minimum Doppler velocity (only shown outlines), since the radiation characteristics and vertical structures of the BBC are compared. For this radar RHI, the direction represents the property of strong echo cells. The time lag of the AVHRR/NOAA-10 and Doppler radar scan is

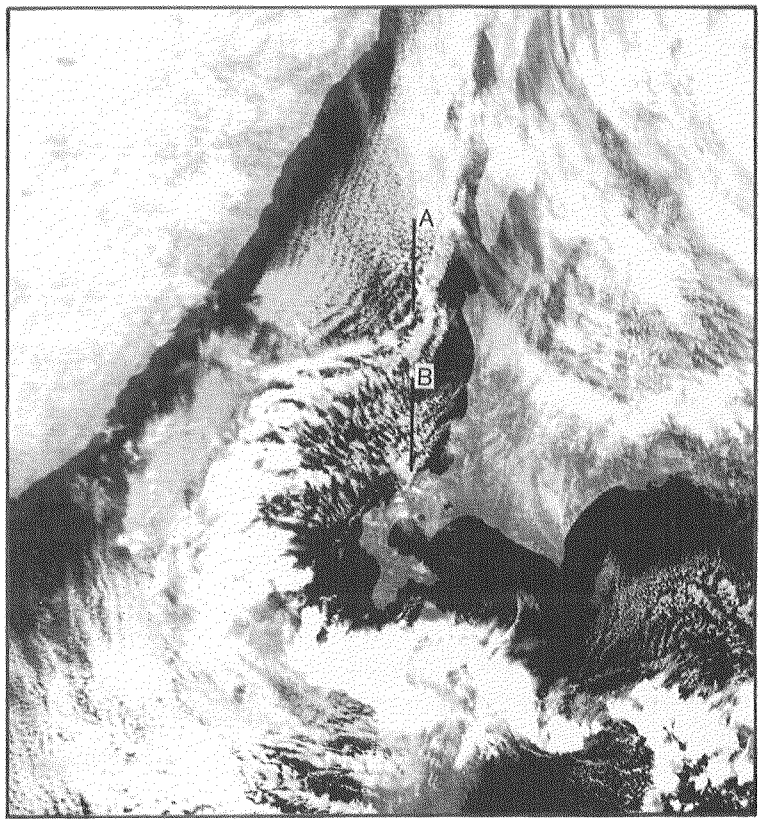

Fig. 5. AVHRR/NOAA-10 channel 4 (IR) imagery at 0646 JST on 28 January 1991. The area of IR imagery illustrates the same region of Fig. 1 (left panel). *Line A* and *Line B* outside of the broad band snow cloud (BBC) are investigated in section 4.3.

also ignored for this BBC on 28 January 1991. Convective echoes are exhibited on the radar RHI ranges of 12~20 km and 40~48 km with a relatively strong intensity at this time. The convective regions show the T3-T4 value is close to 0 K ($\pm$1 K). In the above section 3.2, the existence of the convective snow cloud is discussed by the value (the T3-T4 is 0$\pm$1 K).

Furthermore, the radiation property on this cross section is represented in Fig. 9 as a scatter diagram. The scatter plots identified as convective regions (corresponding to *Sector C* as expressed in Fig. 2) occupy 64% in total. This fact suggests that the BBC which originated near Rebun Island is composed of convective clouds over the ocean. On the other hand, the scatter plots of coldly anvil regions (recognized as *Sector A* in Fig. 2) are 36%. The latter attribution

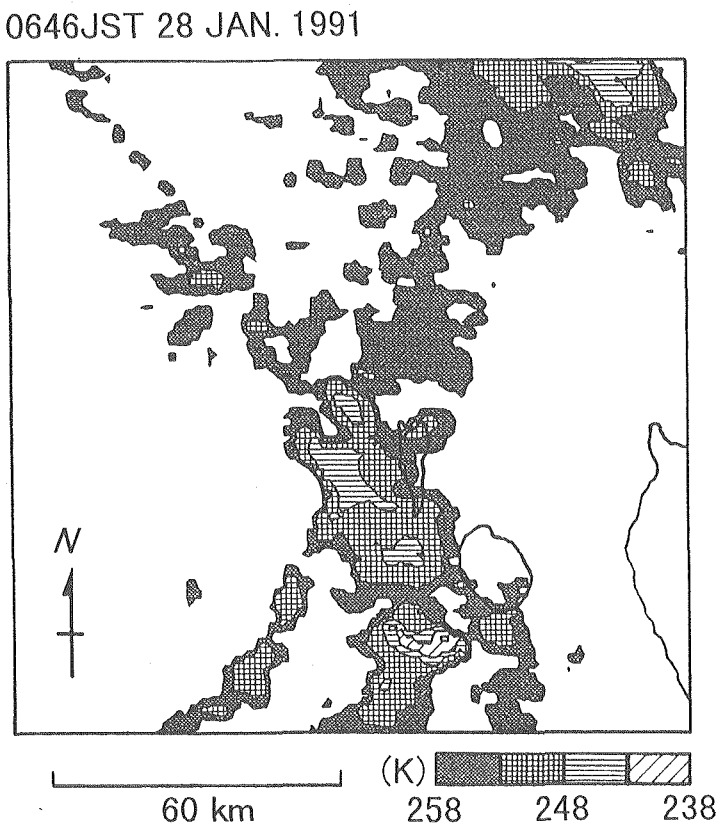

Fig. 6. Detailed AVHRR/NOAA-10 channel 4 (IR) imagery around the radar site (Rebun Island) at 0646 JST on 28 January 1991. The image represents the same area of Fig. 1 (right panel).

reflects the cloud portions south of convective clouds. Since the region corresponding to the *Sector B* in Fig. 2 is not plotted, only convective cloud systems are dominant in the initial BBC formation around the Rebun Island.

4.3 Radiations and cloud systems on initial BBC

In order to discuss the cloud system in a wide range of the initial BBC formations, scatter diagrams of radiative characteristics are shown in Fig. 10. Figure 10(a) and (b) describe the northern part (*Line A* in Fig. 5) and the southern part (*Line B* in Fig. 5) respectively, which are outside the BBC. For the north feature of the BBC, the share of convective regions (corresponding to *Sector C* in Fig. 2) is 22% on the *Line A* and that of cirrus and/or cold anvil

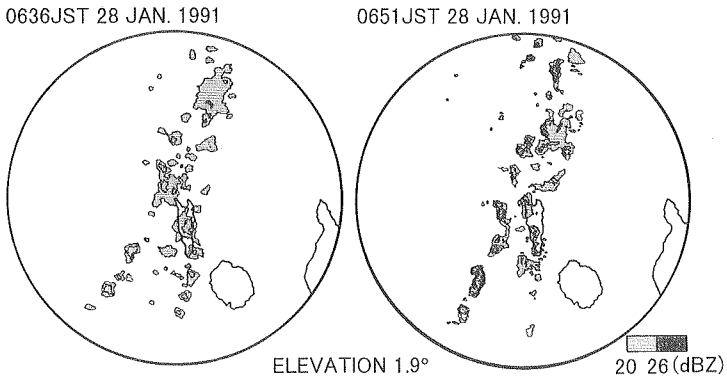

Fig. 7. The X-band Doppler radar reflectivity (dBZ) of PPI (Plan Position Indicator) with the circle of 60 km in radius at the elevation angle of 1.9°. The times at 0636 JST and 0651 JST on 28 January 1991 are the nearest AVHRR/NOAA-10 satellite scanning over the radar site. The reflectivity contours are drawn for 20 dBZ (outer) and 26 dBZ (inner).

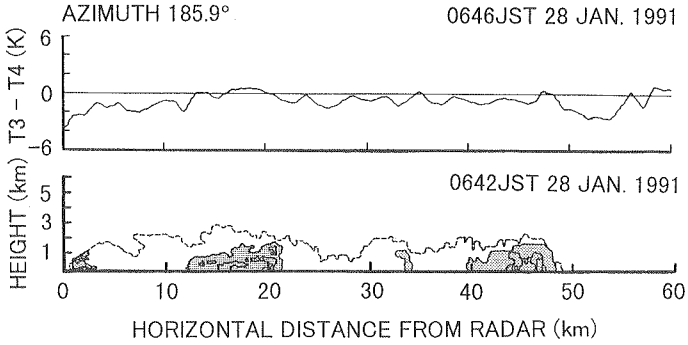

Fig. 8. The brightness temperature differences (upper panel) on AVHRR/NOAA-10 channel 3 and 4 (T3-T4 ; K) and the RHI (Range Height Indicator) of the X-band Doppler radar (lower panel) with the reflectivity (dBZ ; solid contours and shaded areas over 20 dBZ) and the minimum Doppler velocity (dashed line) at the southward radar site (an azimuth angle is 185.9°).

regions (the *Sector A* in Fig. 2) occupy 64% in T4 less than 258 K. As the region corresponding to *Sector A* in Fig. 2 is predominant on *Line A*, the cloud system on the northern region outside of the BBC is considered to be composed of strongly streak clouds with convective cells under the winter monsoon outbreak.

In Fig. 10(b) to the south and outside of the BBC, on the other hand, the convective region (the *Sector C* in Fig. 2) and the cirrus and/or cold anvil region (the *Sector A* in Fig. 2) yield 46% and 49% on the *Line B* in Fig. 5 respectively. These radiative properties on the scatter diagram in the cloud region are similar to those of Fig. 9 and the results expressed section in 4.2. The cloud system in

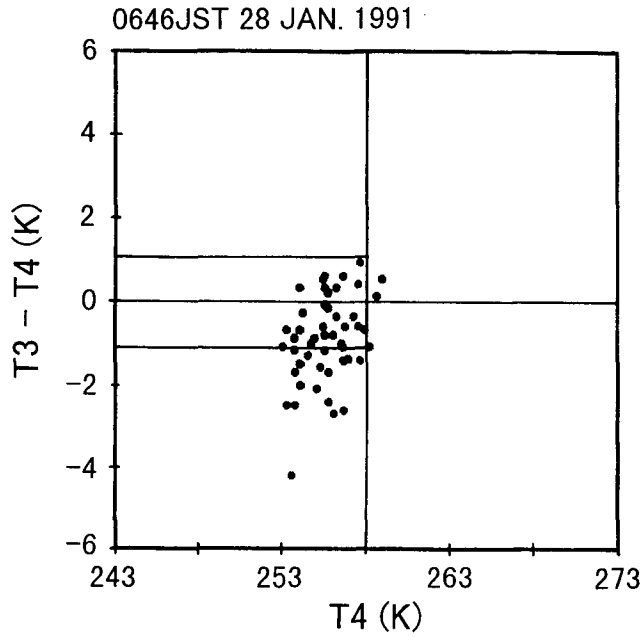

Fig. 9. Same as Fig. 2 but for the scatter diagram of the same cross line in Fig. 8.

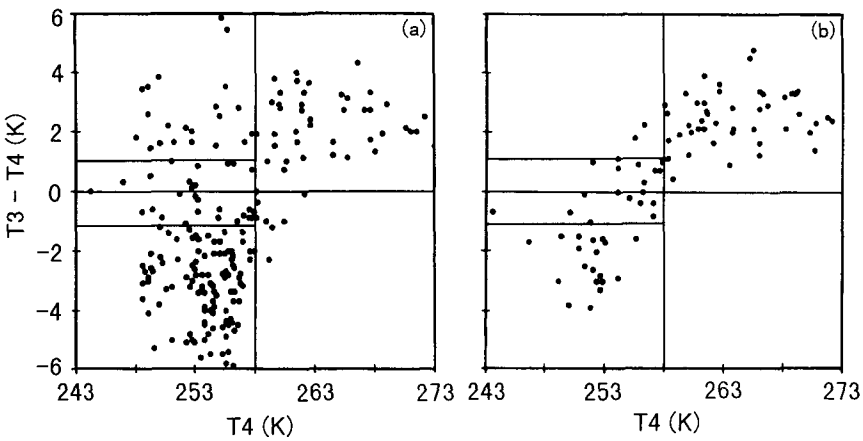

Fig. 10. Same as Fig. 2 but for the scatter diagrams that (a) and (b) describe the northern part (*Line A* in Fig. 5) and the southern part (*Line B* in Fig. 5) outside of the BBC respectively.

the southern region is mainly composed of convective clouds. Specifically, the obvious differences which indicate radiative characteristics in two locations of the *Line A* and *Line B* outside of the BBC are related to the formation of clouds, the convective activity and the stage of the BBC.

5. Discussion

As shown in the previous section, radiative features of the BBC and snow clouds in the northern and southern parts out of it were diagnosed. The radiation characteristics of the northern region (as expressed by *Line A* in Fig. 5 and the diagram in Fig. 10(a)) is attributed to strong streak clouds under the winter monsoon outbreak with predominant cirrus and/or cold anvil regions including convective cells. The southern region (*Line B* in Fig. 5 and the diagram in Fig. 10(b)) is comprised of convective snow clouds. The remarkable differences in radiative properties between the northern and southern regions outside the BBC are considered to mirror the stage of cloud development and/or the depth of the mixing layers: the thickness of the mixing layer of the northern region is larger than that of the southern region.

The radiative features of the BBC conformed to that of developing convective clouds. Katsumata et al. (1996) attempted to investigate the initial structures of a BBC by combining data from SSM/I (the Special Sensor Microwave Imager), a satellite-borne microwave radiometer, and radars. They described that a BBC around the Rebun Island performed correspondingly a behavior similar to the narrow cold frontal band of extratropical cyclones (Hobbs and Biswas, 1979; James and Browning, 1979). The BBC on 28 January 1991 is also considered to be the narrow cold frontal type counting the convective properties of the cloud region in the southern area outside of the BBC.

The comparison of radiative characteristics in different regions revealed the conformity of convective radiation properties and a strong radar reflectivity (expressed the section 4.2), and suggests that the present method is effective for identifying the convective snow cloud and estimating cloud stages: the convective cloud region has cloud-top temperatures less than 258 K, and brightness temperature differences (T3-T4) of AVHRR/NOAA-10 channels 3 and 4 close to 0 K (± 1 K); the cloud stage is diagnosed with negative values on T3-T4 less then -1 K around convective clouds.

6. Conclusions

Initial structures and cloud systems of a broad band snow cloud (BBC) formed off Hokkaido Island, Japan are investigated by AVHRR/NOAA-10 and single X-band Doppler radar data. In this paper, we have examined a method to distinguish convective cells and anvils of snow clouds in the BBC with satellite radiances. The procedure presents utilizing an actual scatter diagram corresponding to brightness temperature differences (T3-T4) of the AVHRR/NOAA-10 channels 3 and 4 plotted as the function of channel 4 brightness temperature (T4). On the basis of the theoretically radiative background, the radiative features of a snow cloud and BBC are compared with their cloud systems.

A typical case of the initial BBC on 28 January 1991 is selected among radar observations carried out from 16 to 28 January 1991 on Rebun Island. The radar echoes on the PPI consists of several convective cells. The configuration coincides well with the AVHRR/NOAA-10 T4 imagery. The alignment of strong echoes over 20 dBZ corresponds to the region of the lower T4. Next, in order to understand the relations between the radiative properties on the cloud-top and its cloud systems, a vertical cross section of the southern echo cells is inspected. The convective regions show that the T3-T4 value yields close to 0 K (± 1 K).

Radiative features of the BBC and snow clouds in the northern and southern parts outside of the BBC were also explored. The radiation characteristics of the northern region are attributed to strong streak clouds under the winter monsoon outbreak with predominant cirrus and/or cold anvil regions including convective cells. The southern region is comprised of convective snow clouds. Specifically, the remarkable differences in radiative properties between the northern and southern regions outside of the BBC are considered to mirror the stages of cloud developments and/or the depth of the mixing layers. The thickness of the mixing layer of the northern region is larger than that of the southern region.

As the comparison of radiative characteristics in different regions near the BBC revealed the conformity of convective radiation properties and a strong radar reflectivity, we suggest that the present procedure is extremely effective for identifying the convective snow cloud and estimating the cloud development stages.

Acknowledgments

The authors express their thanks to Dr. Yoshio Asuma, Meteorological Laboratory, Graduate School of Science, Hokkaido University, for his helpful discussion. The authors extend their thanks to Mr. Akio Takemoto and the students of the laboratory for their assistance in the observation. Thanks are also extended to Rebun Town Hall for their cooperation and the provisions for installations and facilities, and to the Japan Meteorological Agency for permission to use meteorological data. The AVHRR/NOAA data set was recorded by the Center for Atmospheric and Oceanic Studies, Faculty of Science, Tohoku University. The authors express special thanks to Prof. Hiroshi Kawamura, Tohoku University, for providing the AVHRR/NOAA data set. The authors also would like to thank Dr. Yasumasa Kodama, Faculty of Science and Technology, Hirosaki University, for helping satellite data conversion. This study was partly supported by Grant-in-Aid (Nos. 02201102, 03201104 and 04201102) of the Ministry of Education, Science, Sports and Culture of Japan.

References

Adler, R.F. and A.J. Negri, 1988. A satellite infrared technique to estimate tropical convective and stratiform rainfall. J. Appl. Meteor., **27**, 30-51.

Allen, R.C., Jr., P.A. Durkee and C.H. Wash, 1990. Snow/cloud discrimination with multispectral satellite measurements. J. Appl. Meteor., **29**, 994-1004.

Arkin, P.A., 1979. The relationship between fractional coverage of high cloud and rainfall accumulations during GATE over the B-scale array. Mon. Wea. Rev., **107**, 1382-1387.

Asai, T., 1988. Meso-scale features of heavy snowfalls in Japan Sea coastal regions of Japan. Tenki, **35**, 156-161 (in Japanese).

Fujiyoshi, Y., K. Tsuboki, H. Konishi and G. Wakahama, 1988. Doppler radar observation of convergence band cloud formed on the west coast of Hokkaido Island (I): Warm frontal type. Tenki, **35**, 427-439 (in Japanese).

Fujiyoshi, Y., Y. Kodama, K. Tsuboki, K. Nishimura and N. Ono, 1996. Structures of cold air during the development of a broad band cloud and a meso-β-scale vortex: Simultaneous two-point radiosonde observations. J. Meteor. Soc. Japan, **74**, 281-297.

Giraud, V., C. Buriez, Y. Fouquart, F. Parol and G. Seze, 1997. Large-scale analysis of cirrus clouds from AVHRR data: Assessment of both a microphysical index and the cloud-top temperature. J. Appl. Meteor., **36**, 664-675.

Hobbs, P.V. and K.R. Biswas, 1979. The cellular structure of narrow cold-frontal rainbands. Quart. J. Roy. Meteor. Soc., **105**, 723-727.

Inoue, T., 1985. On the temperature and effective emissivity determination of semi-transparent cirrus clouds by bi-spectral measurements in the 10 μm window region. J. Meteor. Soc. Japan, **63**, 88-98.

James, P.K. and K.A. Browning, 1979. Mesoscale structure of line convection at surface cold fronts. Quart. J. Roy. Meteor. Soc., **105**, 371-382.

Katsumata, M., H. Uyeda and K. Kikuchi, 1996. Internal structure of cloud bands off the

west cast of Hokkaido Island, Japan, analyzed with SSM/I and radar data. Proceedings of 12th ICCP, Zurich, 573-576.

Kidder, S.Q. and H. Vonder Harr, 1995. Satellite meteorology : An introduction. Academic Press, 466 pp.

Kobayashi, F., K. Kikuchi and T. Motoki, 1987. Studies on the convergence band cloud formed in the mid-winter seasons on the west coast of Hokkaido Island, Japan (I). Geophys. Bull. Hokkaido Univ., **49**, 341-357 (in Japanese with English summary).

Kodama, Y., T. Nakayama and N. Osaki, 1995. Precipitation variations over the northeastern part of Japan on a scale of one or several hundred kilometers during winter monsoon periods. Tenki, **42**, 85-96 (in Japanese).

Lauritson, L., G.J. Nelson and F.W. Porto, 1979. Data extraction and calibration of TIROS-N/NOAA radiometers. NOAA Tech. Memo. NESS **107**, U.S. Dept. of Commerce, Washington, DC, 73 pp.

Liou, K.N., 1980. An introduction to atmospheric radiation. Academic Press, 404 pp.

Liou, K.N., 1992. Radiation and cloud processes in the atmosphere, Oxford Univ. Press, 487 pp.

Nagata, M., 1993. Meso-β-scale vortices developing along the Japan-Sea polar-airmass Convergence Zone (JPCZ) cloud band: Numerical simulation. J. Meteor. Soc. Japan, **71**, 43-57.

Okabayashi, T. and M. Satomi, 1971. A study on the snowfall and its original clouds by the meteorological radar and satellite (Part I). Tenki, **18**, 573-581 (in Japanese).

Sasaki, H. and T. Satomura, 1991. Numerical experiment on convergence cloud bands over the northern part of the Japan Sea. J. Meteor. Soc. Japan, **69**, 375-388.

Satoh, S., Y. Fujiyoshi, G. Wakahama, R. Shirooka and H. Uyeda, 1992. Dual Doppler radar observation of convergence band cloud. Proceedings of 11th ICCP, Zurich, 628-631.

Takemoto, A., H. Uyeda, K. Kikuchi and N. Osaki, 1998. An observational study on the generation and development of meso-β and γ scale band clouds in winter around Rebun Island, Hokkaido, Japan. J. Fac. Sci., Hokkaido Univ., Ser. VII, (Geophysics), **11**, 89-115.

Taylor, V.R., and L.L. Stowe, 1984. Atlas of reflectance patterns for uniform earth and cloud surfaces (NIMBUS-7 ERB-61 Days). NOAA Tech. Rep. NESDIS-10, U.S. Dept. of Commerce, Washington, DC, 66 pp.

Tsuboki, K., Y. Fujiyoshi and G. Wakahama, 1989. Doppler radar observation of convergence band cloud formed on the west coast of Hokkaido Island (II): Cold frontal type. J. Meteor. Soc. Japan, **67**, 985-989.

Uyeda, H., A. Takemoto, N. Osaki and K. Kikuchi, 1992. Structures of convective snow bands at formation stage in northwest coast of Hokkaido, Japan. Proceedings of 11th ICCP, Montreal, 624-627.

Wu, M.C., 1987. A method for remote sensing the emissivity, fractional cloud cover, and cloud top temperature of high-level, thin clouds. J. Climate Appl. Meteor., **26**, 225-233.

Yamanouchi, T., K. Suzuki and S. Kawaguchi, 1987. Detection of clouds in Antarctica from infrared multispectral data of AVHRR. J. Meteor. Soc. Japan, **65**, 949-962.